doi:10.1093/brain/awq368 Brain 2011: 134; 863–878 | 863

BRAIN
A JOURNAL OF NEUROLOGY

A voxel-based morphometry study of grey matter loss in fragile X-associated tremor/ataxia syndrome

Ryu-ichiro Hashimoto,[1] Alireza K. Javan,[1] Flora Tassone,[2,3] Randi J. Hagerman[2,4] and Susan M. Rivera[1,2,5]

1 Center for Mind and Brain, University of California Davis, Davis, CA 95618, USA
2 M.I.N.D. Institute, University of California Davis, Sacramento, CA 95817, USA
3 Department of Biochemistry and Molecular Medicine, University of California, Davis, Sacramento, CA 95616, USA
4 Department of Paediatrics, University of California Davis Medical Center, Sacramento, CA 95817, USA
5 Department of Psychology, University of California Davis, Davis, CA 95618-5412, 95616, USA

Correspondence to: Dr Susan M. Rivera,
Center for Mind and Brain,
University of California Davis,
267 Cousteau Place,
Davis, CA 95618-5412, USA
E-mail: srivera@ucdavis.edu

Fragile X-associated tremor/ataxia syndrome is a neurodegenerative disorder that primarily affects older male premutation carriers of the fragile X mental retardation gene. Although its core symptoms are mainly characterized by motor problems such as intention tremor and gait ataxia, cognitive decline and psychiatric problems are also commonly observed. Past radiological and histological approaches have focused on prominent neurodegenerative changes in specific brain structures including the cerebellum and limbic areas. However, quantitative investigations of the regional structural abnormalities have not been performed over the whole brain. In this study, we adopted the voxel-based morphometry method together with regions of interest analysis for the cerebellum to examine the pattern of regional grey matter change in the male premutation carriers with and without fragile X-associated tremor/ataxia syndrome. In a comparison with healthy controls, we found striking grey matter loss of the patients with fragile X-associated tremor/ataxia syndrome in multiple regions over the cortical and subcortical structures. In the cerebellum, the anterior lobe and the superior posterior lobe were profoundly reduced in both vermis and hemispheres. In the cerebral cortex, clusters of highly significant grey matter reduction were found in the extended areas in the medial surface of the brain, including the dorsomedial prefrontal cortex, anterior cingulate cortex and precuneus. The other prominent grey matter loss was found in the lateral prefrontal cortex, orbitofrontal cortex, amygdala and insula. Although the voxel-wise comparison between the asymptomatic premutation group and healthy controls did not reach significant difference, a regions of interest analysis revealed significant grey matter reduction in anterior subregions of the cerebellar vermis and hemisphere in the asymptomatic premutation group. Correlation analyses using behavioural scales of the premutation groups showed significant associations between grey matter loss in the left amygdala and increased levels of obsessive–compulsiveness and depression, and between decreased grey matter in the left inferior frontal cortex and anterior cingulate cortex and poor working memory performance. Furthermore, regression analyses revealed a significant negative effect of CGG repeat size on grey matter density in the dorsomedial frontal regions. A significant negative correlation with the clinical scale for the severity of fragile X-associated tremor/ataxia syndrome was found in a part of the vermis. These observations reveal the anatomical patterns of the neurodegenerative process that underlie the motor, cognitive and psychiatric problems of fragile X-associated tremor/ataxia syndrome, together with incipient structural abnormalities that may occur before the clinical onset of this disease.

Received July 22, 2010. Revised October 16, 2010. Accepted November 3, 2010

Keywords: fragile X-associated tremor/ataxia syndrome; movement disorder; voxel based morphometry; cerebellum; atrophy

Abbreviations: FXTAS = fragile X-associated tremor/ataxia syndrome; *FMR1* = fragile X mental retardation gene 1; PFX^+ = *FMR1* premutation carriers with FXTAS; PFX^- = *FMR1* premutation carriers without FXTAS; SCL-90-R = symptom Checklist-90 Revised

Introduction

Abnormalities of the fragile X mental retardation gene (*FMR1*) are associated with a diverse range of behavioural and clinical phenotypes depending on the type of mutation. Expansions of the CGG trinucleotide repeats in the full mutation range (>200 CGG) are the genetic cause of the *FMR1* protein deficiency that underlies the fragile X syndrome (Fu *et al.*, 1991; Pieretti *et al.*, 1991; Verkerk *et al.*, 1991). Smaller expansions of 55–200 repeats are referred to as the premutation. Because the premutation does not cause severe protein (*FMR1* protein) deficiency as observed in the full mutation, it was initially thought not to be associated with a particular psychological or neurocognitive phenotype. However, recent studies have accumulated evidence for several cognitive and psychiatric problems in adult and child carriers of premutation alleles (Franke *et al.*, 1998; Johnston *et al.*, 2001; Hagerman and Hagerman, 2002; Moore *et al.*, 2004; Cornish *et al.*, 2005; Farzin *et al.*, 2006; Hessl *et al.*, 2007).

Fragile X-associated tremor/ataxia syndrome (FXTAS) is probably the most clinically significant central nervous system phenotype of the *FMR1* premutation. FXTAS is a late-onset neurodegenerative disorder primarily affecting older male premutation carriers. Although it is principally characterized as a movement disorder involving intention tremor and gait ataxia, cognitive decline and psychiatric problems are also commonly observed (Hagerman *et al.*, 2001; Jacquemont *et al.*, 2003; Bacalman *et al.*, 2006; Bourgeois *et al.*, 2009). While its pathogenetic mechanism is still unclear, an RNA toxic 'gain-of-function' model has been proposed based on several observations (Hagerman *et al.*, 2001; Hagerman and Hagerman, 2004), including: the presence of elevated *FMR1* messenger RNA among premutation carriers without clear indications of abnormal *FMR1* protein expression (Tassone *et al.*, 2000; Kenneson *et al.*, 2001); the presence of *FMR1* messenger RNA within intranuclear inclusions (Greco *et al.*, 2006), one of the hallmarks of FXTAS (Tassone *et al.*, 2004); and premature neuronal cell death in culture combined with dysregulation of several proteins secondary to elevated messenger RNA (Chen *et al.*, 2010, Garcia-Arocena and Hagerman, 2010).

Previous studies have revealed anatomical abnormalities in several structures of the FXTAS brain. Particularly, abnormalities of the cerebellum have been demonstrated in multiple methodologies. In a clinical MRI study, the middle cerebellar peduncle sign was described as one of the most characteristic neuroradiological features of FXTAS (Brunberg *et al.*, 2002). Cerebellar abnormalities were confirmed by post-mortem histological studies that identified several neuropathological features, including Purkinje cell decreases and spongiform changes (Greco *et al.*, 2002, 2006). Significant loss in whole cerebellar volume has been revealed in the male patients with FXTAS (Cohen *et al.*, 2006), which was further replicated in the female patients in a milder form (Adams *et al.*, 2007). However, there have been no studies that attempted to identify the foci of neurodegeneration within the cerebellum. This point is crucial given the fact that there are multiple functionally different subregions in the cerebellum (Stoodley and Schmahmann, 2009) and therefore structural changes in different subregions may make distinct contributions to motor, cognitive and psychiatric problems in FXTAS. Similarly, regionally selective abnormalities in the cerebral cortex are entirely unclear, although the aforementioned MRI volumetric study revealed significant loss of the whole cerebral volume in the patients with FXTAS (Cohen *et al.*, 2006).

Previous behavioural studies revealed patterns of neurocognitive and psychological deficits of FXTAS (Cornish *et al.*, 2005, 2008; Grigsby *et al.*, 2006, 2007), which provide motivations for examining the possible regionally selective abnormalities in cortical and subcortical structures in the FXTAS brain. One study applied an extensive neuropsychological test battery to male premutation carriers with and without FXTAS and reported that, whereas language and visuospatial/attention functions were relatively spared, patients with FXTAS displayed profound deficits of executive cognitive functions, working memory and declarative verbal memory and learning (Grigsby *et al.*, 2008). Several studies replicated significant deficits of executive functions and working memory not only in FXTAS but also in unaffected premutation carriers (Cornish *et al.*, 2008, 2009). For psychological symptoms, it has been reported that major psychiatric features of FXTAS include increased anxiety, depression, disinhibition and apathy (Berry-Kravis *et al.*, 2007*b*; Bourgeois *et al.*, 2007, 2009). In a large-scale study examining self-reported psychological symptoms of patients with FXTAS and unaffected premutation carriers, the level of the obsessive–compulsiveness was elevated even in unaffected premutation carriers, whereas psychological symptoms of FXTAS extended into other domains, including anxiety and depression (Hessl *et al.*, 2005). Although one recent region of interest-based volumetric study reported a significant correlation between the right hippocampal volume and the severity of anxiety-related psychological symptoms among female patients with FXTAS (Adams *et al.*, 2010), there has been no study that systematically investigated foci of structural abnormalities that may underlie major neurocognitive and psychological problems in individuals with FXTAS and unaffected premutation carriers.

In this study, we adopted the voxel-based morphometry method to examine the regional grey matter loss in the *FMR1* premutation carriers with and without FXTAS. Voxel-based morphometry is an automated analysis for assessment of the regional volumetric change over the whole brain (Ashburner and Friston, 2000). For a set of brain regions whose deficits can be responsible for neurocognitive and psychological deficits of the *FMR1* premutation carriers, we performed region of interest analyses to examine associations between the grey matter abnormalities in those regions and the severity of the behavioural problems

(refer to 'Materials and Methods' section for selection of regions of interest.) Simple voxel-based regression analyses using either CGG repeat size or level of *FMR1* messenger RNA of premutation carriers were also performed to examine the effects of the genetic molecular variables on the grey matter abnormality over the whole brain. Lastly, the same simple regression analysis was applied using a clinical scale for assessment of the FXTAS severity to identify brain regions showing progressive neurodegeneration correlated with the development of FXTAS.

Materials and methods

Participants

We examined the brains of a total of 83 male participants between the ages of 40 and 80 years, 28 healthy control participants, 31 participants with the premutation with FXTAS (PFX^+), and 24 participants with the premutation without FXTAS (PFX^-). In this study, the premutation range was defined as those with a CGG repeat size of between 55 and 200. CGG repeat size was <45 in all the healthy control cases, so that there was no participant whose CGG repeat was within the 'grey zone' (45–54 CGG repeats). Participant demographic information is shown in Table 1. The group of PFX^+ was significantly older than the other two groups [$F(2, 80) = 5.19$, $P = 0.008$]. Twenty-six controls, 27 PFX^+ and 22 PFX^- were assessed for full, verbal and performance-scale IQ using the Wechsler Adult Intelligence Scale (Third Edition). According to one-way analysis of variance (ANOVA), a significant main effect of group was found for performance IQ [performance IQ: $F(2, 67) = 4.16$, $P = 0.019$; full-scale IQ: $F = 2.69$, $P = 0.075$; verbal IQ: $F = 1.24$, $P = 0.30$], with healthy control and PFX^- individuals having higher performance IQs than those with PFX^+ ($P < 0.05$). Participants with the premutation were recruited through pedigree analysis of families containing probands with fragile X syndrome. Controls were recruited from the families and the local community through the University of California Davis Medical Centre. Neurological examinations on all healthy control participants were normal, including absence of tremor and ataxia. A signed, written informed consent was obtained according to the Declaration of Helsinki. The protocol was approved by the institutional review board at the University of California, Davis.

Molecular genetic data

Genomic DNA was isolated from peripheral blood lymphocytes using standard methods (Puregene® Kit; Gentra Inc). For Southern blot analysis, 5–10 μg of isolated DNA was digested with EcoRI and NruI. Hybridization was performed using the *FMR1* genomic digoxygenin-labelled StB12.3 probe. Genomic DNA was also amplified by polymerase chain reaction using primers 'c' and 'f' (Fu *et al.*, 1991). Hybridization was performed with a digoxygenin-end-labelled oligonucleotide probe $(CGG)^{10}$. Analysis and calculation of the repeat size for both Southern blot and polymerase chain reaction analysis were carried out using an Alpha Innotech FluorChem 8800 Image Detection System (Tassone *et al.*, 2008).

Total cellular RNA was purified from 3–5 ml of peripheral blood using standard methods (Purescript® kits, Gentra Inc.; Trizol®, BRL). All quantification of *FMR1* messenger RNA were performed using a 7900 Sequence detector (PE Biosystems) as previously described (Tassone *et al.*, 2000).

Assessment of clinical severity of fragile X-associated tremor/ataxia syndrome

For participants with CGG repeat count within the premutation range, a trained physician (RJH) scored the severity of FXTAS on a scale ranging from 0–6 as described by our previous studies (Bacalman *et al.*, 2006; Adams *et al.*, 2007). This seven-point staging scale measures functional impairment as follows: 0 = normal functioning; 1 = subtle or questionable tremor or balance problems with no interference in activities of daily living; 2 = minor but clear tremor or balance problems producing minor interference with activities of daily living; 3 = moderate tremor or balance problems with at least occasional falls and significant interference in activities of daily living; 4 = severe tremor or balance problems requiring the use of a cane or walker; 5 = use of a wheelchair on a daily basis and 6 = bedridden. Premutation carriers with FXTAS scores of 0 or 1 were placed in the PFX^- group, while those with FXTAS scores of 2–5 were designated as PFX^+, meeting clinical criteria for the diagnosis of FXTAS established initially by Jacquemont *et al*. (2003).

Clinical data acquisition

To examine the relationship between grey matter loss in specific brain regions and behavioural problems of the *FMR1* premutation carriers, PFX^+ and PFX^- individuals were administered a series of examinations for assessing their psychological and cognitive functioning.

Psychological assessment

The Symptom Checklist-90-Revised (SCL-90-R), a standardized self report inventory of current psychological symptoms (Derogatis, 1994), was used for assessing the severity of psychological symptoms

Table 1 Statistics on participant demographic data

	Healthy controls ($n = 28$)		Premutation with FXTAS (PFX^+) ($n = 31$)		Premutation without FXTAS (PFX^-) ($n = 24$)	
	Mean (SD)	Range	Mean (SD)	Range	Mean (SD)	Range
Age (years)	58.2 (11.1)	40–79	65.2 (7.45)	47–79	58.1 (10.0)	41–78
Full scale IQ	118.6 (16.7)	84–148	108.1 (14.7)	85–136	115.8 (16.5)	83–152
Performance IQ	116.5 (14.3)	89–144	104.9 (14.8)	79–128	115.4 (16.3)	91–155
Verbal IQ	117.0 (17.3)	76–148	109.5 (14.5)	87–135	113.8 (17.4)	78–142
FXTAS score	NA		2.97 (0.98)	2–5	0.35 (0.48)	0–1
CGG repeat	28.6 (4.37)	17–34	93.8 (18.1)	59–130	94.9 (30.6)	55–166
FMR1 messenger RNA	1.29 (0.29)	0.63–1.85	3.32 (0.81)	1.75–5.25	3.15 (0.95)	1.86–5.14

NA = data not available; SD = standard deviation.

in premutation participants. In this instrument, 90 items are clustered into the symptom dimensions of somatization, obsessive–compulsive, interpersonal sensitivity, depression, anxiety, hostility, phobic anxiety, paranoid ideation and psychoticism. Among these dimensions, we selected obsessive–compulsive, depression and anxiety as particularly relevant dimensions to psychiatric problems of premutation carriers based on our previous study using the SCL-90-R that revealed high scores for obsessive–compulsiveness (Hessl *et al.*, 2005), and our previous meta-analysis finding of the elevated level of anxiety and depression among premutation carriers (Bourgeois *et al.*, 2009). We obtained scores in 26 PFX^+ cases and 17 PFX^- cases as follows: obsessive–compulsive = 64.71 ± 11.27 (mean ± standard deviation) in PFX^+ and 55.76 ± 7.88 in PFX^-; depression = 63.21 ± 13.16 in PFX^+ and 54.79 ± 9.46 in PFX^-; anxiety = 58.38 ± 12.10 in PFX^+ and 51.23 ± 8.27 in PFX^-. PFX^+ showed significantly higher scores in the three dimensions than PFX^- (obsessive–compulsive: $t_{41} = 2.843$, $P = 0.007$; depression: $t = 2.275$, $P = 0.028$; anxiety: $t = 2.128$, $P = 0.039$).

Cognitive assessment

We assessed the executive functions and working memory in premutation carriers based on previous behavioural studies. We used the 'Behavioural Dyscontrol Scale 2 as a measure of executive cognitive functioning. The Behavioural Dyscontrol Scale consists of nine items and measures the capacity for executive cognitive function that addresses self-regulation over voluntary and goal-directed motor behaviours (Kaye *et al.*, 1990). We used the sum of the nine sub-item scores as a measure of executive function. As a measure of working memory, we used the sum of working memory subscales (Working Memory Score) of the Wechsler Adult Intelligence Scale. We obtained Behavioural Dyscontrol Scale from 15 PFX^+ participants and 18 PFX^- participants, and the working memory score from 20 PFX^+ participants and 16 PFX^- participants. Mean and standard deviations were: Behavioural Dyscontrol Scale = 14.13 ± 5.51 in PFX^+ and 20.05 ± 4.09 in PFX^-; working memory score = 32.0 ± 7.36 in PFX^+ and 34 ± 8.0 in PFX^-. PFX^+ showed significantly worse Behavioural Dyscontrol Scale ($t_{31} = 3.538$, $P = 0.001$) whereas there was no significant difference in working memory ($t_{34} = 0.938$, $P = 0.355$).

Image acquisition

MRI data were acquired on a 1.5T GE Signa Horizon LX NV/I MRI system package (GE Medical Systems, Milwaukee, WI, USA) using a phased array whole-head coil. A high resolution T_1-weighted spoiled grass gradient (SPGR) 3D MRI sequence with 124 contiguous horizontal slices (repetition time = 8.7 ms; echo time = 1.8 ms; in-plane resolution = 0.86 × 0.86 mm; slice thickness = 1.3 mm; flip angle = 15°) was administered. During the scan, a custom-built head holder was used to prevent movement.

Voxel-based morphometry analysis

MRI data were processed using Statistical Parametric Mapping software (SPM5) (Wellcome Department of Cognitive Neurology, London, UK) and its 'VBM5' toolbox (http://dbm.neuro.uni-jena.de/vbm/vbm5-for-spm5) running on MATLAB version 7.4.0 (The Mathworks, Inc., Natick, MA, USA). Image registration, tissue classification and bias correction were performed under the 'unified segmentation' framework (Ashburner and Friston, 2005). In this framework, the first 40 iterations of the initial segmentation estimation are followed by 40 iterations of bias filed correction and finally 20 iterations are made for warping the prior image to the data. This iterated scheme is repeated until no significant changes occur. Standard International Consortium for Brain Mapping grey matter/white matter templates were used for normalization. All images were modulated by correcting for non-linear warping effects and smoothed with a 12 mm full-width at half-maximum smoothing kernel. Grey matter differences between groups were assessed using the general linear model on a voxel-by-voxel basis over the whole brain volume. Because of the significant age difference between groups (Table 1), we included the age of each participant as the covariate of non-interest. Statistical threshold was set at family-wise error rate corrected $P < 0.05$ and a spatial extent threshold (k) of 100 voxels was used for all the contrasts. We first performed the contrast of healthy controls versus PFX^+. For the contrast of PFX^- versus PFX^+ and for that of healthy controls versus PFX^-, we used an inclusive mask of healthy controls versus PFX^+ (family-wise error-corrected $P < 0.05$, $k = 100$) to increase the statistical power for detecting the intermediate changes that may occur in PFX^-.

Region of interest analysis for cerebellar subregions

Given past neuropathological and neuroradiological findings (Brunberg *et al.*, 2002; Greco *et al.*, 2002, 2006), significant grey matter loss in the cerebellum is expected for the patients with FXTAS. In order to characterize abnormalities within the cerebellum in detail, we parcellated the cerebellum into subregions using the WFU PickAtlas (Maldjian *et al.*, 2003) in which the cerebellum is divided into nine subregions in each hemisphere (lobule III, IV/V, VI, VIIB, VIII, IX, X, Crus I and Crus II) and eight subregions in the vermis (vermis I/II, III, IV/V, VI, VII, VIII, IX and X) (Schmahmann *et al.*, 1999; Lasek *et al.*, 2006). Using the modulated individual grey matter image, we calculated the mean grey matter density of voxels in each subregion. Because of the significant age difference among groups, the individual mean grey matter value was adjusted for the effect of age by calculating the residual after a linear fit of age. The residual value of each subregion in each participant was fed into a two-way ANOVA of Group and Subregion.

Correlation analysis using neurocognitive and psychological measures

A number of past studies replicated crucial involvement of the lateral and medial prefrontal cortex in executive cognitive processes as well as working memory (Buckner and Koutstaal, 1998; Cabeza and Nyberg, 2000). A recent meta-analysis of functional imaging studies of the cerebellum showed that areas in the Crus I and lobule VI of the hemisphere are most reliably activated in tasks for executive processes and working memory (Stoodley and Schmahmann, 2009). It turned out that, in the comparison between healthy controls and PFX^+, prominent grey matter loss was identified in the anterior cingulate cortex and left inferior frontal cortex in the cerebral cortex. In the cerebellum, the bilateral Crus I and lobe VI were also profoundly affected (Fig. 1). Therefore, we hypothesized that grey matter loss in these regions may be responsible for impairments of executive functions and working memory in premutation carriers. To test this hypothesis, we calculated correlation between the mean grey matter density of each of these four regions of interest and behavioural measures of the

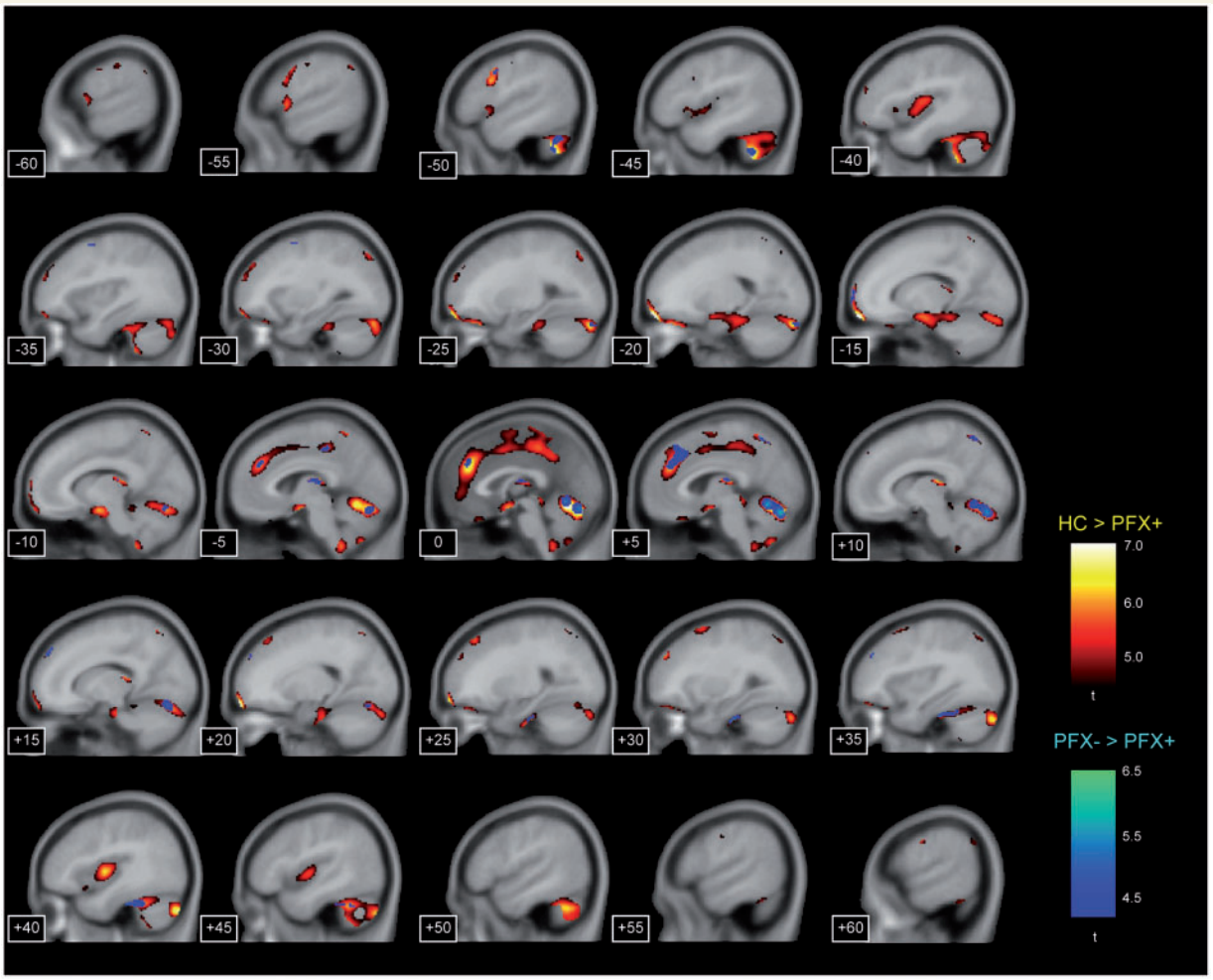

Figure 1 Significant grey matter reduction of FXTAS (PFX^+) identified by comparison either with healthy controls (HC) or with unaffected premutation carriers (PFX^-) in sagittal views. The contrast of healthy control versus PFX^+ is shown in the yellow-red colour scale and the one of PFX^- versus PFX^+ is shown in the deep-light blue scale. The numbers at the bottom left corner indicate the *x*-axis coordinates of sagittal sections. The statistical threshold was set at $P < 0.05$ (family-wise error rate-corrected). The spatial extent threshold was set at 100 voxels.

Behavioural Dyscontrol Scale and the working memory score. To focus on parts of regions of interest where significant atrophy in PFX^+ was identified, voxels in each region of interest was defined by the combination of two binary masks: (i) the contrast map of healthy controls versus PFX^+ (family-wise error-corrected $P < 0.05$, $k = 100$) and (ii) the WFU PickAtlas (Maldjian *et al.*, 2003). The mean grey matter density of each region of interest was calculated from all voxels in the individual modulated grey matter image that satisfied both binary masks. The WFU PickAtlas mask of each region of interest was generated as follows: left inferior frontal cortex = 'Frontal_Inf_Oper_L' + 'Frontal_Inf_Tri_L'; anterior cingulate cortex = 'Cingulum_Ant_L' + 'Cingulum_Ant_R'; left (right) Crus I and lobule VI = 'Cerebelum_Crus1_L(R)' + 'Cerebellum_6_L(R)'. The individual mean grey matter value was then adjusted for the effect of age by calculating the residual value after a linear fit of age. We used the residual for the calculation of correlation with either Behavioural Dyscontrol Scale or working memory score. To adjust for the multiple statistical tests for each scale (four regions of interest/statistical tests per scale), the Benjamini-Hochberg method was implemented, with the false discovery rate set at 5% (Benjamini and Hochberg, 1995).

There has been evidence that anxiety-related symptoms (e.g. obsessive–compulsive disorder and general anxiety) involve abnormalities in the amygdala, insula, anterior cingulate cortex and orbitofrontal cortex (Paulus and Stein, 2006; Etkin and Wager, 2007; Chamberlain *et al.*, 2008). Past studies indicated that neural correlates of depression involve the hippocampus, in addition to the amygdala and anterior cingulate cortex (Soares and Mann, 1997; Sheline, 2000). In the cerebellum, the aforementioned review study indicated that vermal lobule VII is involved in emotional processing by forming the cerebellar-limbic circuitry (Stoodley and Schmahmann, 2009). Because the contrast of healthy controls versus PFX^+ revealed prominent grey matter loss in these regions except for the right amygdala and the right hippocampus (Fig. 1), we performed correlation analyses between the mean intensity of each of these regions of interest and subscales of the SCL-90-R (obsessive–compulsive, depression and anxiety). We extracted the mean intensity of each region of interest using the contrast map of healthy controls versus PFX^+ and the WFU PickAtlas in the

same way as was done in the correlation analysis of executive function and working memory. The WFU PickAtlas mask of each region of interest was generated as follows: left amygdala = 'Amygdala_L'; anterior cingulate cortex = 'Cingulum_Ant_L' + 'Cingulum_Ant_R'; left (right) insula = 'Insula_L(R)'; left (right) orbitofrontal cortex = 'Frontal_Mid_Orb_L(R)' + 'Frontal_Inf_Orb_L(R)'; the vermal lobule VII = 'Vermis_7'. Correlation with obsessive–compulsiveness and anxiety was tested for the left amygdala, anterior cingulate cortex, left and right insula, left and right orbitofrontal cortex, and vermal lobule VII. Correlation with depression was tested for the left amygdala, left hippocampus, anterior cingulate cortex and the vermal lobule VII. The Benjamini-Hochberg method was used for the adjustment of multiple statistical tests for each subscale in the SCL-90-R (seven tests for obsessive–compulsive and anxiety, and four tests for depression).

Regression analysis using *FMR1* molecular variables and fragile X-associated tremor/ataxia syndrome severity scale

In order to examine effects of *FMR1* molecular variables on grey matter, we performed a voxel-based simple regression analysis over the whole brain using either the CGG repeat size or *FMR1* messenger RNA level. We included the age of each participant as the 'nuisance' covariate in the model. Because there is a systematic difference in the distribution of both molecular variables between healthy controls and the two premutation groups (Table 1), we included the data of the two premutation groups only for this analysis in order to avoid contamination of group (categorical) effects.We also performed the simple regression analysis using the clinical scale for assessment of the FXTAS severity to identify areas showing progressive grey matter reduction caused by the development of FXTAS. We included age as the covariate of non-interest to isolate the effect of clinical severity from the one of age. For this analysis, we used the data from premutation participants whose FXTAS score was $\geqslant 1$. We used the contrast of healthy controls versus PFX$^+$ (family-wise error-corrected $P < 0.05$, $k = 100$) as the inclusive mask in the three simple regression analyses.

Results

Group difference in the whole-brain analysis

For the comparison between healthy controls and PFX$^+$, we found clusters of significant grey matter reduction of PFX$^+$ in multiple brain regions over the cerebrum, cerebellum and subcortical structures (Fig. 1 and Table 2). Particularly prominent grey matter loss was observed in the cerebellum, dorsomedial frontal and parietal regions, orbitofrontal regions, insula, medial temporal regions and lateral prefrontal regions. Significant grey matter increase in FXTAS was mainly found in the bilateral posterior superior/middle temporal gyrus (Table 2). In the comparison between PFX$^+$ and PFX$^-$, we found significant grey matter reduction of PFX$^+$ relative to PFX$^-$ in parts of the cerebellum, dorsomedial prefrontal cortex, and precuneus (Fig. 1 and Table 2). There were no significant voxels showing PFX$^+$ > PFX$^-$. No significant voxels were identified in the comparison between healthy controls and PFX$^-$ in either direction.

Region of interest analyses for cerebellar subregions

A two-way ANOVA (Group × Subregion) for the 26 cerebellar subregions revealed a significant main effect of Group [$F(2, 80) = 9.427$, $P < 0.001$] and interaction effect [$F(50, 2000) = 2.918$, $P < 0.001$]. Follow-up one-way ANOVA was performed for each subregion using the Benjamini-Hochberg method for the adjustment for the multiple tests. We did not observe significant effects of Group in lobules VIII and IX in the vermis, bilateral lobule VIII nor right lobule X in the hemisphere. All other subregions showed a significant main effect of Group ($P < 0.05$; Table 3). According to a *post hoc* test (Tukey's Honestly Significant Difference), there was a significant difference between healthy controls and PFX$^+$ in all of the regions of interest (Table 3). Compared with healthy controls, PFX$^-$ showed significant reduction in lobule I/II of the vermis and in lobule III in the left hemisphere ($P < 0.05$; Fig. 2 and Table 3). Significant differences between PFX$^+$and PFX$^-$ were found in lobules IV/V, VI and VII in the vermis, and lobules IV/V, VI, Crus I and right Crus II in the hemisphere ($P < 0.05$; Fig. 2 and Table 3).

Region of interest-based correlation analysis using neurocognitive and psychological measures

In correlation analysis with Behavioural Dyscontrol Scale, none of the four regions of interest for executive function reached significance using the threshold corrected for multiple comparisons (left inferior frontal cortex: $r = 0.392$, $P = 0.0968$; anterior cingulate cortex: $r = 0.300$, $P = 0.119$; left Crus I/lobule VI: $r = 0.265$, $P = 0.1364$; right Crus I/lobule VI: $r = 0.373$, $P = 0.065$), although left inferior frontal cortex and the right Crus I/lobule VI showed significant correlations at an uncorrected threshold ($P = 0.024$ and $P = 0.032$, respectively). In correlation analysis using the working memory score, we found significant correlations in the anterior cingulate cortex ($r = 0.498$, $P = 0.004$) and the left inferior frontal cortex ($r = 0.518$, $P = 0.005$) at the corrected threshold (Fig. 3). The two cerebellar regions of interest, by contrast, showed no significant correlation (left Crus I/lobule VI: $r = 0.192$, $P = 0.263$; right Crus I/lobule VI: $r = 0.289$, $P = 0.117$) with Behavioural Dyscontrol Scale.

In correlation analysis using the score of the obsessive–compulsive symptom dimension in SCL-90-R, only the left amygdala reached the significant level ($P = 0.0126$; Fig. 3). Although there were several regions of interest for which a significant correlation was observed at the uncorrected threshold (anterior cingulate cortex: $r = -0.358$, $P = 0.018$; left insula: $r = -0.316$, $P = 0.039$; right insula: $r = -0.311$, $P = 0.042$), these regions of interest did not reach significant level after correction (anterior cingulate cortex: $P = 0.064$; left insula: $P = 0.091$; right insula: $P = 0.074$). No other regions of interest showed significant correlation (vermis lobule VII: $r = -0.205$, $P = 0.188$; left orbitofrontal cortex: $r = -0.272$,

Table 2 Significant grey matter differences between groups

Region	Cluster size	x	y	z	z_{max}
Healthy controls > PFX$^+$					
Left and right cerebellar hemispheres, vermis, ventral medial temporal regions	53025	5	−77	−21	6.43
Cingulate cortex, dorsomedial prefrontal cortex, pre-SMA, SMA, precuneus	22729	−1	40	29	5.95
Left insula/frontal operculum	4663	−57	10	1	5.38
Left orbital frontal cortex	4228	−18	62	−19	6.78
Left and right cerebellar lobule IX	3558	−8	−45	−58	5.45
Right insula	2938	41	−6	3	5.75
Thalamus	2076	−2	−19	13	5.69
Left inferior frontal cortex	1876	−51	10	29	5.57
Right orbital frontal cortex	1656	21	65	−16	6.26
Left dorsolateral prefrontal cortex	1213	−33	54	23	4.98
Right superior frontal cortex	743	31	11	62	5.14
	686	23	37	51	5.35
Bilateral gyrus rectus	559	3	29	−29	4.80
Left superior parietal cortex	553	−28	−77	47	5.22
Right superior parietal cortex	341	35	−69	53	4.77
Right premotor cortex	200	59	−5	39	5.08
Left angular gyrus	190	−55	−60	41	4.98
Right angular gyrus	173	62	−58	37	4.75
Left superior frontal cortex	159	−32	4	60	4.81
Left post-central gyrus	148	−61	−24	41	4.73
PFX$^+$ > Healthy controls					
Left superior/middle temporal gyrus	3674	−46	−50	0	5.92
	275	−48	−9	−22	4.78
Right middle temporal gyrus	1560	52	−47	−12	5.40
	239	49	−50	10	4.77
Left lateral occipital gyrus	204	−29	−85	−2	4.74
	135	−33	−73	14	4.74
Left medial orbital gyrus	185	−20	26	−11	4.71
Right middle frontal gyrus	101	30	42	12	4.72
PFX$^-$ > PFX$^+$					
Cerebellar lobules V/VI/VII	5072	5	−78	−22	5.27
Right cerebellar hemisphere VI	1613	30	−23	−36	5.10
Dorsal anterior cingulate/paracingulate	1471	6	30	40	4.65
Left cerebellar hemisphere VIIB/Crus I	841	−48	−53	−47	4.41
Thalamus	625	−4	−18	12	4.30
Right precuneus	355	6	−60	60	4.66
Right dorsomedial prefrontal cortex	257	16	51	42	4.54
Left cerebellar hemisphere Crus I	222	−22	−90	−27	4.20
Left frontal pole	191	−15	69	6	4.12
Right superior frontal cortex	174	33	47	33	4.51
Left premotor cortex	168	−52	6	40	4.34
Left superior frontal cortex	146	−34	4	59	4.61
Left posterior cingulate cortex	135	−5	−31	47	4.08
PFX$^+$ > PFX$^-$					
No significant clusters					
Healthy controls > PFX$^-$					
No significant clusters					
PFX$^-$ > Healthy controls					
No significant clusters					

SMA = supplementary motor area.

$P = 0.091$; right orbitofrontal cortex: $r = -0.277$, $P = 0.101$). In the correlation using the depression symptom dimension, only the left amygdala was significantly correlated using the corrected threshold ($P = 0.019$; Fig. 3). No other regions of interest showed significant correlation after correction (anterior cingulate cortex: $r = -0.264$, $P = 0.116$; left hippocampus: $r = -0.301$, $P = 0.100$; vermis VII: $r = -0.093$, $P = 0.554$), although the left hippocampus showed a marginally significant correlation at the uncorrected threshold ($P = 0.050$). There was no region of interest that showed a significant correlation with anxiety after

Table 3 Group comparisons of age-adjusted grey matter density in the cerebellar subregions

Region	Healthy controls	PFX$^+$	PFX$^-$	*F*-test
Vermis				
Lobule I/II*,***	3.48 ± 1.10	−2.91 ± 1.19	0.59 ± 1.08	$F = 8.42$, $P < 0.001$
Lobule III*	3.32 ± 1.04	−3.26 ± 1.07	0.09 ± 1.08	$F = 10.09$, $P < 0.001$
Lobule IV/V*,**	3.09 ± 1.04	−3.76 ± 1.09	0.87 ± 0.91	$F = 12.19$, $P < 0.001$
Lobule VI*,**	4.93 ± 1.13	−5.66 ± 1.25	1.18 ± 1.27	$F = 20.66$, $P < 0.001$
Lobule VII*,**	3.77 ± 1.12	−4.93 ± 1.31	1.45 ± 1.14	$F = 14.74$, $P < 0.001$
Lobule VIII	2.16 ± 1.16	−2.37 ± 1.61	0.04 ± 1.35	$F = 2.72$, $P = 0.078$
Lobule IX	2.71 ± 1.41	−2.78 ± 1.88	−0.35 ± 1.63	$F = 2.83$, $P = 0.077$
Lobule X*	2.50 ± 1.12	−2.31 ± 1.34	−0.36 ± 1.08	$F = 4.22$, $P = 0.018$
Hemisphere				
Lobule III				
L*,***	3.54 ± 1.04	−3.04 ± 1.12	−0.46 ± 1.13	$F = 9.54$, $P < 0.001$
R*	2.90 ± 0.92	−2.87 ± 0.98	0.01 ± 0.84	$F = 10.22$, $P < 0.001$
Lobule IV/V				
L*,**	3.60 ± 0.95	−3.69 ± 1.16	0.18 ± 1.14	$F = 11.86$, $P < 0.001$
R*,**	2.83 ± 1.03	−3.97 ± 1.31	1.26 ± 0.97	$F = 10.28$, $P < 0.001$
Lobule VI				
L*,**	3.32 ± 0.96	−3.90 ± 1.33	0.66 ± 1.18	$F = 10.11$, $P < 0.001$
R*,**	2.46 ± 0.92	−3.95 ± 1.27	1.55 ± 0.95	$F = 10.75$, $P < 0.001$
Crus I				
L*,**	3.15 ± 0.81	−3.82 ± 1.02	0.74 ± 0.99	$F = 14.76$, $P < 0.001$
R*,**	2.64 ± 0.84	−3.61 ± 1.01	0.96 ± 0.88	$F = 12.98$, $P < 0.001$
Crus II				
L*	2.70 ± 0.82	−3.09 ± 1.22	0.30 ± 1.15	$F = 7.66$, $P < 0.001$
R*,**	2.50 ± 0.79	−2.98 ± 0.95	0.66 ± 0.91	$F = 10.18$, $P < 0.001$
Lobule VIIB				
L*	2.22 ± 0.94	−2.59 ± 1.46	0.20 ± 1.26	$F = 3.91$, $P = 0.029$
R*	2.23 ± 0.96	−2.77 ± 1.24	0.48 ± 1.04	$F = 5.61$, $P < 0.001$
Lobule VIII				
L	1.62 ± 1.02	−1.61 ± 1.68	−0.31 ± 1.37	$F = 1.40$, $P = 0.254$
R	1.42 ± 1.06	−1.91 ± 1.44	0.26 ± 1.05	$F = 1.99$, $P = 0.148$
Lobule IX				
L*	3.04 ± 1.28	−2.62 ± 1.58	−0.65 ± 1.46	$F = 4.06$, $P = 0.027$
R*	3.08 ± 1.21	−2.68 ± 1.65	−0.79 ± 1.21	$F = 4.51$, $P = 0.020$
Lobule X				
L*	1.19 ± 0.52	−0.81 ± 0.70	−0.38 ± 0.70	$F = 4.51$, $P = 0.021$
R	0.99 ± 0.63	−1.14 ± 0.65	0.22 ± 0.70	$F = 2.79$, $P = 0.076$

Age-adjusted grey matter density represents the residual from a linear regression of age over the modulated grey matter density extracted from each subregion. *Significant difference between controls and PFX$^+$ by a *post hoc* test (Tukey HSD). **Significant difference between PFX$^-$ and PFX$^+$. ***Significant difference between healthy controls and PFX$^-$. L = left; R = right.

correction (left amygdala: $r = -0.252$, $P = 0.717$; anterior cingulate cortex: $r = -0.241$, $P = 0.421$; left insula: $r = -0.217$, $P = 0.284$; right insula: $r = -0.212$, $P = 0.242$; left orbitofrontal cortex: $r = -0.222$, $P = 0.355$; right orbitofrontal cortex: $r = -0.208$, $P = 0.210$; vermis VII: $r = -0.154$, $P = 0.324$).

Whole brain regression analyses using *FMR1* molecular variables and clinical scale of fragile X-associated tremor/ataxia syndrome

We performed regression analyses using CGG repeat size and *FMR1* messenger RNA. For the analysis involving CGG repeat size, we found significant negative effects of CGG repeat size in several clusters in the dorsal medial regions including the supplementary motor area and the dorsomedial prefrontal cortex (Fig. 4 and Table 4). No voxels showed a significant positive effect of CGG repeat size. We did not observe a significant correlation with *FMR1* messenger RNA in either direction. In the analysis using the clinical scales of the FXTAS severity, we found significant negative correlations in cerebellar lobule VI/VII and the orbitofrontal cortex (Fig. 5 and Table 4). No significant positive correlations were observed.

Discussion

Brain abnormalities in PFX$^+$ has been demonstrated in previous MRI volumetric studies based on gross anatomical parcellation as

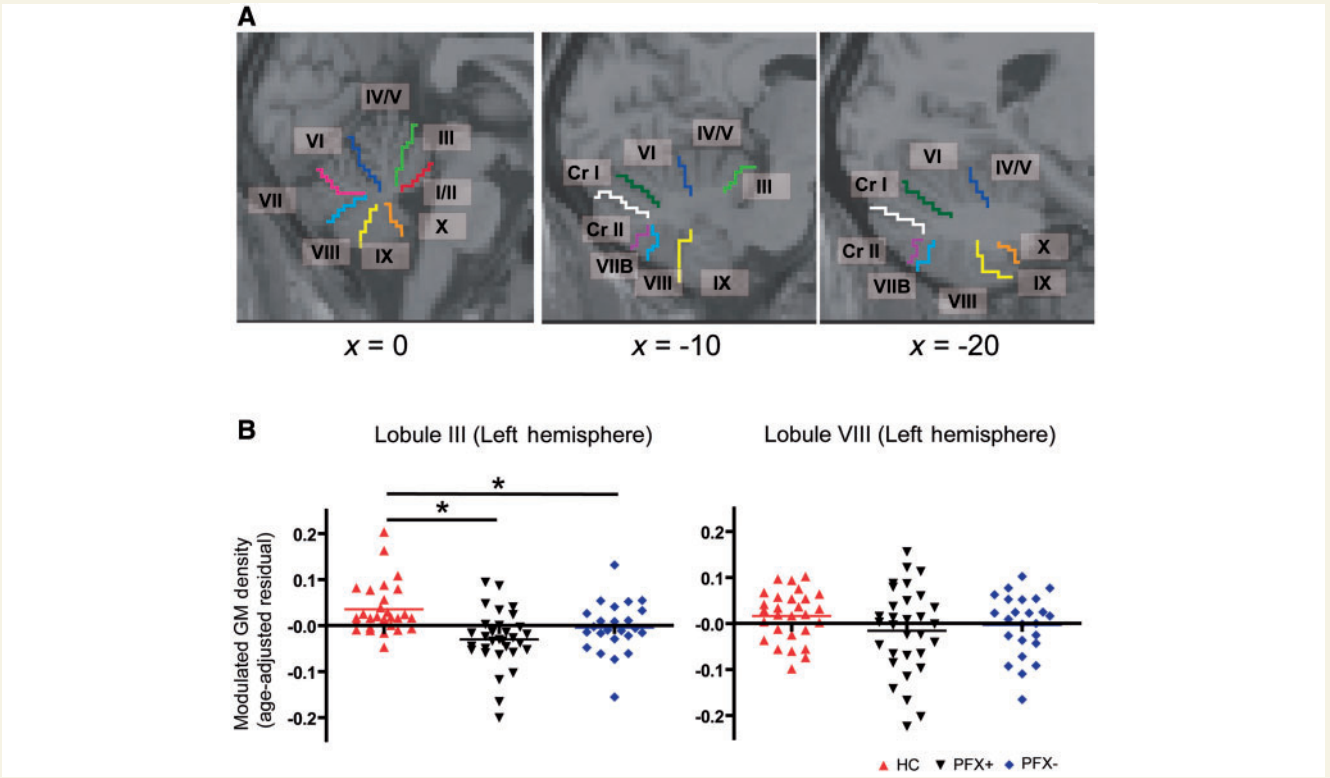

Figure 2 Region of interest analyses of the cerebellar subregions. (**A**) Sagittal views showing cerebellar subregions as determined by the WFU PickAtlas (Maldjian *et al.*, 2003). In the most medial section ($x = 0$), the eight subregions in the vermis are shown (lobules I/II, III, IV/V, VI, VII, VIII, IX and X). The nine subregions in the hemisphere (lobules III, IV/V, VI, VIIB, VIII, IX, X, Crus I and Crus II) are shown in the lateral sections ($x = -10$ and $x = -20$). (**B**) Comparisons of grey matter (GM) density among the three groups in selected cerebellar subregions. Significant difference between two groups is shown by an asterisk. The *y*-axis represents the residual from a linear regression of age over the mean modulated grey matter density extracted from each subregion.

well as clinical MRI investigations (Brunberg *et al.*, 2002; Cohen *et al.*, 2006; Adams *et al.*, 2007, 2010). However, systematic investigations of possible regionally selective abnormalities have not been performed. To our knowledge, this study represents the first demonstration of a spatial pattern of grey matter reduction in the PFX$^+$ brain using voxel-based morphometry. We identified significant grey matter reduction in multiple regions, particularly in the cerebellum, the dorsomedial frontal-parietal regions, the medial temporal regions and the insula. Correlation analysis using the behavioural measurements of the premutation groups indicated that psychological symptoms and working memory deficits of *FMR1* premutation carriers are associated with grey matter loss in the left amygdala and in the left inferior frontal cortex and anterior cingulate cortex, respectively. Regression analyses using *FMR1* molecular variables showed a significant contribution of CGG repeat size to the grey matter reduction in the dorsomedial frontal regions. Furthermore, progressive grey matter loss correlated with the severity of FXTAS symptomatology was also revealed in a part of the cerebellum and in the orbitofrontal cortex. These findings identify the pattern of anatomical abnormalities in *FMR1* premutation carriers that might provide morphological bases for behavioural problems of this population.

Consistent with the past observations, both the whole-brain voxel-based morphometry analysis and the region of interest analyses revealed profound grey matter loss in the cerebellum of PFX$^+$. Significant grey matter reduction was widespread, affecting almost the entire cerebellum except for some subregions in the inferior posterior lobe such as the lobule VIII. In particular, grey matter reductions in the anterior subregions of the vermis and hemispheres were highly significant (Fig. 2). The anterior vermis has been shown to be critical for the regulation of the postural equilibrium while standing (Diener *et al.*, 1989; Ouchi *et al.*, 1999). Severe atrophy in this region of the cerebellum therefore may be directly responsible for gait ataxia, one of the core clinical symptoms of PFX$^+$. We suggest that analysis using behavioural scales for the severity of ataxia, such as the International Cooperative Ataxia Rating Scale, would be necessary to test this hypothesis. It is important to note that significant grey matter reduction was identified in several subregions in the anterior vermis and hemisphere even among PFX$^-$ (Table 3). This observation raises the possibility that degeneration in this region may be the initial pathological process before clinical signs of FXTAS. Significant grey matter loss was also found in several subregions of the posterior vermis. Previous neuropsychological studies described cerebellar cognitive affect syndrome resulted from damage to the posterior lobe (Schmahmann and Sherman, 1998). A recent meta-analysis of functional imaging studies indicated that areas around the vermis lobule VII are recruited with

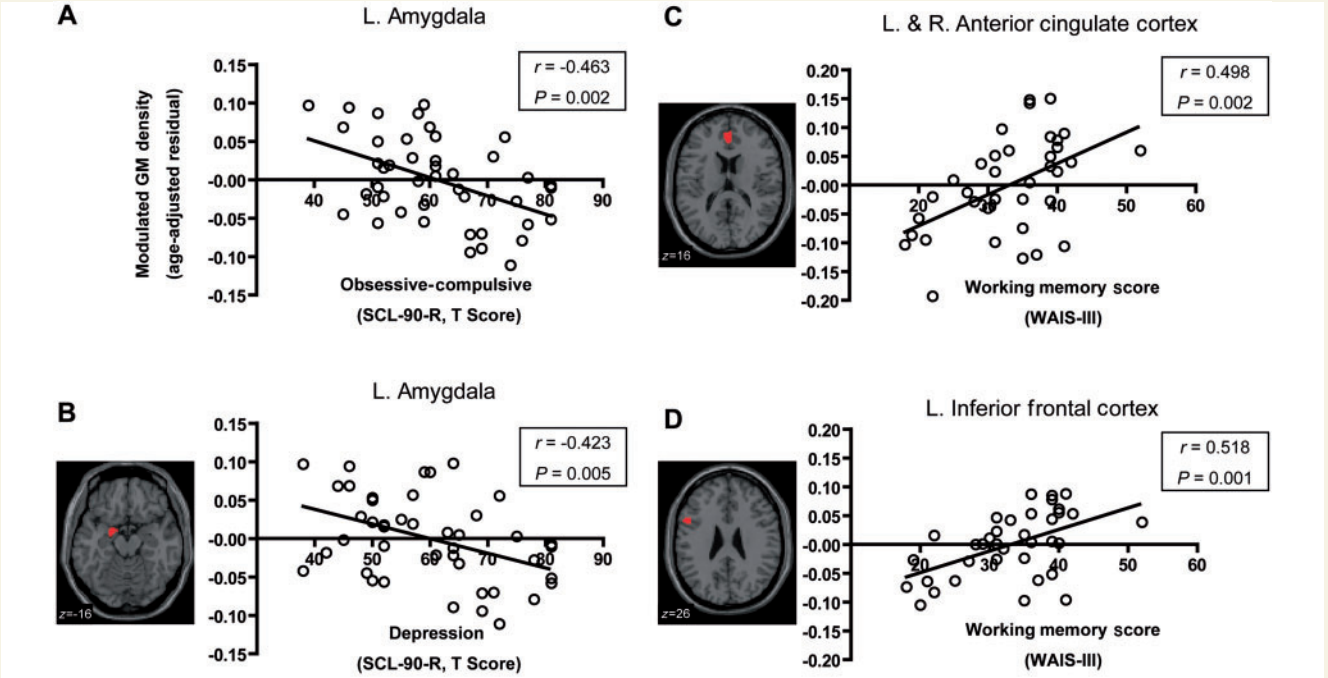

Figure 3 Significant association of grey matter (GM) density in regions of interest with cognitive and psychological scales in premutation carriers. (**A** and **B**) Relations between grey matter density in the left amygdala and self-reported psychological symptoms of obsessive–compulsive (**A**) and depression (**B**) on the SCL-90-R. (**C** and **D**) Relations between the sum of the working memory subscales in Wechsler Adult Intelligence Scale (Third Edition) and the grey matter density in the anterior cingulate cortex (**C**) and left inferior frontal cortex (**D**). Correlation coefficient and *P*-value (uncorrected) are noted. The correlations were found to be significant after correction for multiple comparisons. L = left; R = right.

high probability in tasks of emotional processing (Stoodley and Schmahmann, 2009). Although these findings suggest that significant abnormality of this subregion may be related to psychiatric problems in FXTAS, this possibility was not supported by our correlation analysis that failed to show significant association between the level of depression, anxiety or obsessive–compulsiveness in SCL-90-R and grey matter reduction in this region.

In the cerebellar hemispheres, large grey matter reductions in PFX$^+$ were observed in parts of the neocerebellum, including Crus I, Crus II and lobule VI. According to the aforementioned meta-analysis of cerebellar activation, these neocerebellar regions, particularly the boundary between Crus I and lobule VI, are frequently activated in executive function and working memory tasks (Stoodley and Schmahmann, 2009), which suggests that abnormalities in these cerebellar subregions may contribute to impaired executive and working memory processes in PFX$^+$. However, the present correlation analysis using the Behavioural Dyscontrol Scale and the working memory score did not support this possibility except for the trend-level correlation between the right Crus I/lobule VI volume and the Behavioural Dyscontrol Scale score. Because executive functions comprise various cognitive processes, it is necessary to examine possible relevance with other behavioural tests of executive functions. Compared with these subregions, grey matter reductions in several posterior subregions were less pronounced. In particular, we did not find evidence of significant abnormality of the hemisphere lobule VIII, a subregion that has been shown to be most severely impaired in spinocerebellar ataxia 17 (SCA17), another neurodegenerative disorder caused by a single gene mutation (Lasek *et al.*, 2006). This dissociation is interesting given the phenotypic overlap between this disease and PFX$^+$. Among the posterior subregions, the lobule IX showed significant grey matter loss. This region has been suggested to form the cerebellar node of the 'default-mode' network (Habas *et al.*, 2009). Grey matter loss in this region may thus be related to highly significant abnormalities of cortical nodes of this network, such as the dorsomedial prefrontal cortex and precuneus (Fig. 1).

The comparison between the healthy controls and PFX$^+$ revealed profound grey matter atrophy in several cortical and subcortical regions outside of the cerebellum. In particular, a cluster of significant reduction was identified over the extended areas in the medial surface of the brain between the frontal and parietal regions (Fig. 1). This huge cluster comprises multiple regions including the dorsal anterior cingulate/paracingulate cortex, dorsomedial prefrontal cortex, supplementary motor area, middle and posterior paracingulate cortex and precuneus (Table 2). The most prominent grey matter loss was centred in the dorsal anterior cingulate cortex. Previous functional imaging and brain lesion studies have shown that the anterior cingulate cortex is implicated in both cognitive and emotional processing (Bush *et al.*, 2000). In the cognitive domain, activation of this area has been found under executive cognitive and working memory tasks that require

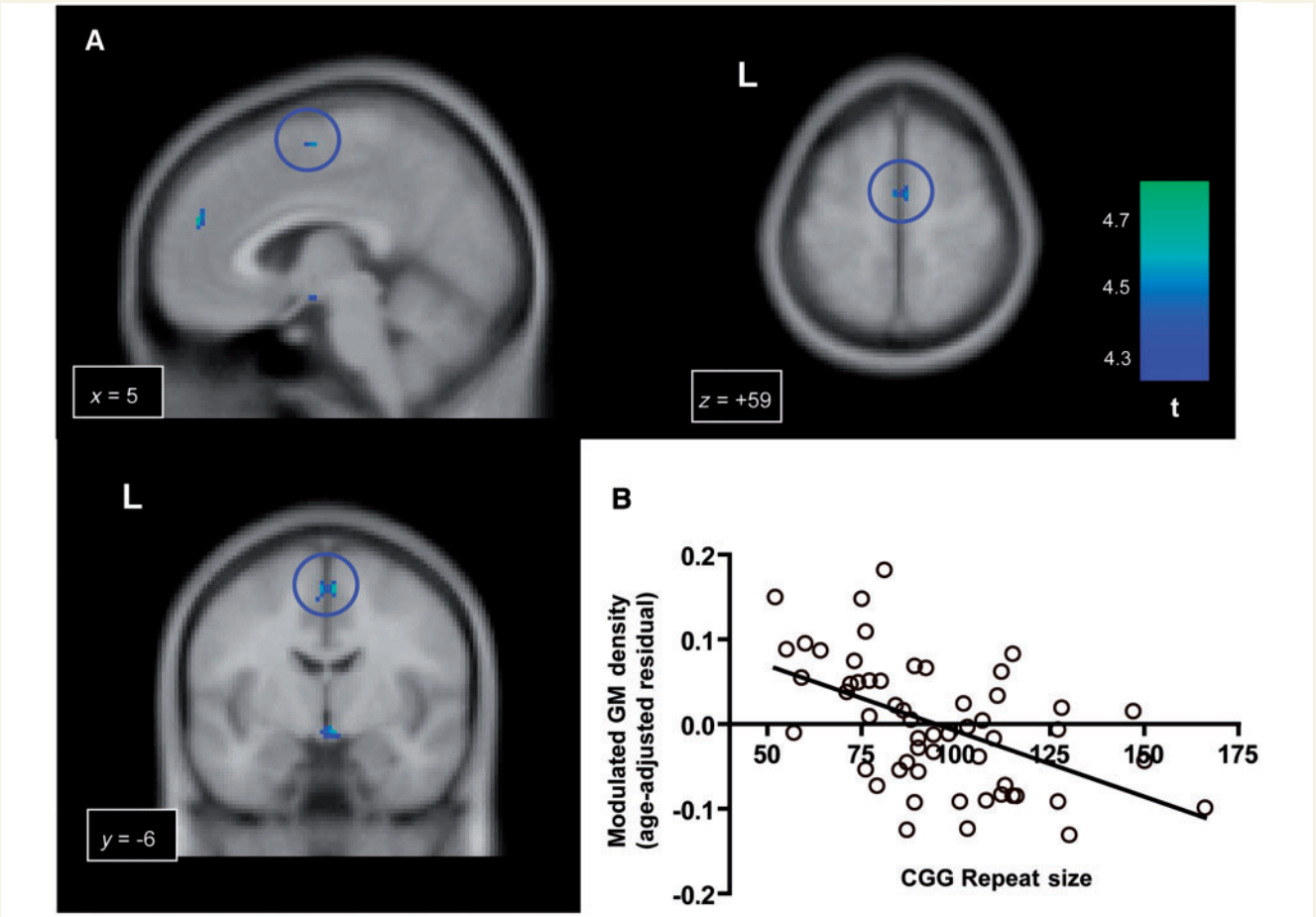

Figure 4 Significant negative effect of the CGG repeat size on the grey matter (GM) density in the *FMR1* premutation carriers. (**A**) Clusters of voxels in the dorsal medial regions showing significant negative correlation with the CGG repeat size. The blue circles indicate the largest cluster in the supplementary motor area in the sagittal, coronal and axial views. (**B**) The plot of CGG repeat size and the grey matter density at a voxel of the highest *t*-value in the supplementary motor area (x, y, $z = 5, -6, 59$). The *y*-axis represents the residual from a linear regression of age over the modulated grey matter density at this coordinate.

Table 4 Regression analysis using CGG repeat size and FXTAS severity scale

Region	Size	*x*	*y*	*z*	z_{max}
CGG repeat size					
Supplementary motor area	283	5	−6	59	4.26
		−3	−5	55	4.20
Mammillary body/anterior ventral hypothalamus	282	3	−5	−11	4.23
Right orbitofrontal cortex	165	16	69	−9	4.33
Left dorsomedial prefrontal cortex	144	−4	28	48	4.25
		−4	49	30	4.11
		−4	40	41	4.09
Right cerebellar hemisphere lobule IX	142	−13	−42	−54	4.35
Right anterior cingulate/paracingulate cortex	109	5	50	25	4.28
FXTAS severity scale					
Right cerebellar vermis lobule VI/VII	639	4	−78	−23	4.66
Right orbitofrontal cortex	398	16	69	−11	4.63

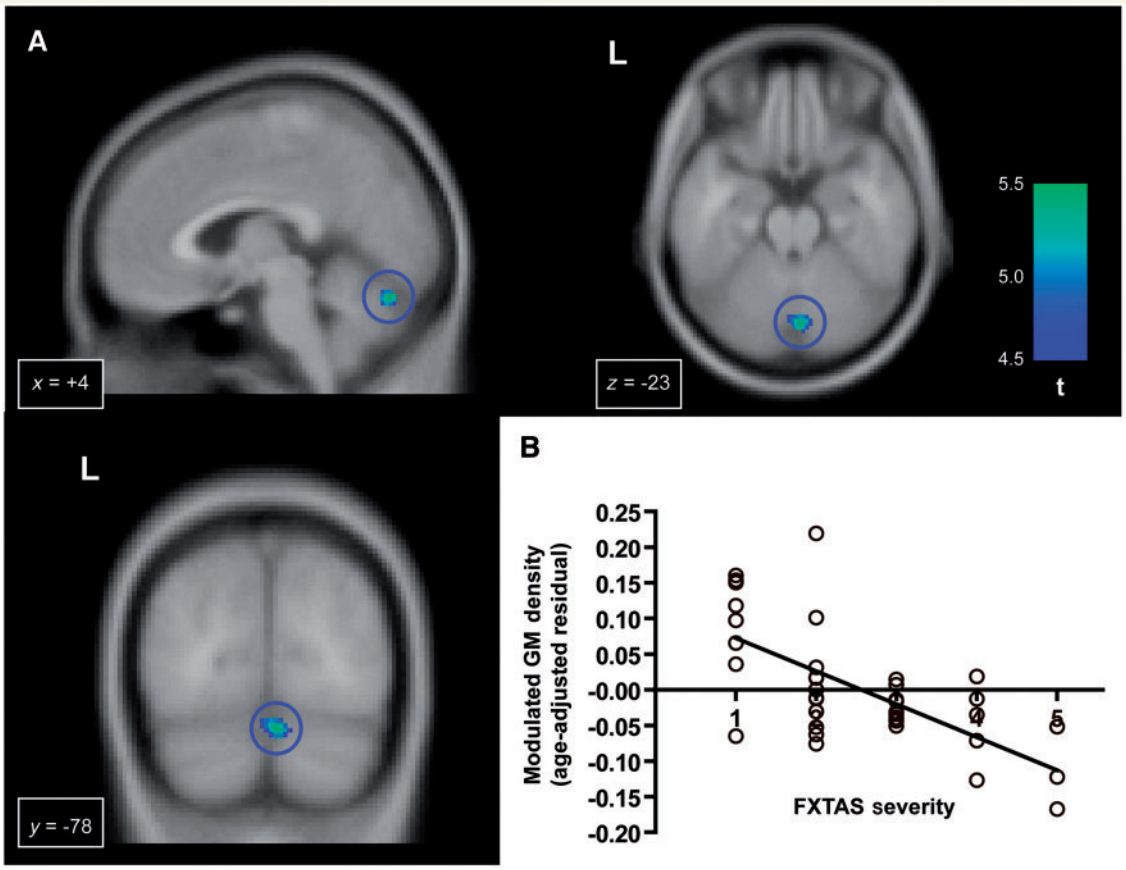

Figure 5 Progressive grey matter (GM) loss correlated with the severity of FXTAS. (**A**) Significant negative correlation with a clinical scale for assessment of the FXTAS severity in the vermis (shown in the blue circles). (**B**) The plot of the FXTAS severity and the grey matter density at a voxel of the highest *t*-value in the vermis (x, y, $z = 4, -78, -23$).

attention, cognitive efforts and performance monitoring (Smith and Jonides, 1999; Paus, 2001). The anterior cingulate cortex is also a part of the network for decision making and social behaviour by forming reciprocal connectivity with the amygdala, orbitofrontal cortex and ventral striatum (Vogt *et al.*, 1995; Cavada *et al.*, 2000; Beckmann *et al.*, 2009). Within this network, it has been proposed that the anterior cingulate cortex plays a crucial role in selection of action, especially that which involves effort (Rushworth *et al.*, 2007). Therefore, dysfunction of this area might be particularly related to impairments of effortful executive and working memory processes and apathetic symptoms of this disease (Bacalman *et al.*, 2006). The present study lent support for this view by showing a significant correlation between anterior cingulate cortex volume and working memory score (Fig. 3). Further studies are needed to examine whether apathy-related symptoms are associated with structural abnormalities in this region.

The cluster of significant grey matter reduction also extended into the adjacent regions such as the dorsomedial prefrontal cortex, pre-supplementary motor area and supplementary motor area (Fig. 1 and Table 2). The medial dorsal prefrontal cortex and precuneus are crucial nodes of the default-mode network (Gusnard and Raichle, 2001; Raichle *et al.*, 2001). Although the function of this network remains to be clarified, past studies proposed that it is involved in episodic memory retrieval, self-reflection and stream-of-consciousness (Greicius *et al.*, 2003; Cavanna and Trimble, 2006). Functional abnormalities of this network have been found in several psychiatric conditions including autism (Kennedy *et al.*, 2006; Monk *et al.*, 2009). It is possible that structural abnormalities of the medial dorsal prefrontal cortex and the precuneus contribute to the memory problem and the development of psychiatric episodes in PFX$^+$. We also found clusters of significant negative correlations with the CGG repeat size in the dorsal medial frontal cortex (Fig. 4 and Table 4) suggesting a significant gene dosage effect of *FMR1* on grey matter in this part of the brain. This further supports the influence of the CGG repeat number on the severity of clinical involvement. Past studies found particularly strong correlation of the CGG repeats with the FXTAS phenotypes including overall motor impairment (Leehey *et al.*, 2007), the age of onset of tremor and ataxia (Tassone *et al.*, 2007), severity of white matter disease and degree of brain atrophy (Loesch *et al.*, 2005; Cohen *et al.*, 2006), severity of neuropathic signs (Berry-Kravis *et al.*, 2007*b*), degree of neuropathy as measured by nerve conduction studies (Soontarapornchai *et al.*, 2008), reduced cerebellar volume (Adams *et al.*, 2007), the percent of inclusions and age at death (Greco *et al.*, 2006), and the

amplitude of electrophysiological response to word processing (Olichney *et al.*, 2010).

Significant grey matter loss was also observed in the bilateral orbitofrontal cortex (Fig. 1 and Table 2). Past neuropsychological studies have shown that patients with cortical damage to this area display impulsive behaviours (Bechara *et al.*, 2000). A recent functional MRI study of patients with obsessive–compulsive disorder and their unaffected close relatives proposed that abnormality of the orbitofrontal cortex may be endophenotype of obsessive–compulsive disorder (Chamberlain *et al.*, 2008). Further, a recent review proposed that this area is important for subjective pleasantness/hedonic processing (Kringelbach, 2005). Given these proposals, it is tempting to associate grey matter reduction of this structure with psychiatric symptoms of disinhibition, obsessive–compulsiveness and impassivity/apathy of PFX$^+$ (Hessl *et al.*, 2005; Bacalman *et al.*, 2006; Bourgeois *et al.*, 2009). However, we did not find significant correlation of the grey matter volume and the level of obsessive–compulsiveness. It remains to be tested whether there is any association with the severity of disinhibition and apathy. We note that, in the voxel-based morphometry analysis, this area is known to be particularly sensitive to misregistration and normalization error. Therefore, we suggest that the structural abnormalities in the orbitofrontal cortex need to be replicated using different methodologies such as manual tracing (Nakamura *et al.*, 2008) and cortical thickness measurements (Kuperberg *et al.*, 2003).

Grey matter loss in PFX$^+$ was clearly observed in the bilateral insula. A classic review described multiple functional roles of insular cortex including the sensory, motor and cognitive domains (Augustine, 1996). In our analysis, foci of grey matter loss were located in the posterior part, although signs of the milder grey matter loss in the anterior part were also observed when a more liberal statistical threshold was used (false discovery rate corrected $P < 0.05$, not reported). Recent functional anatomical studies of both primates and humans highlighted the insula's role in interoception, the sense of physiological condition of the body including the visceral, hunger, pain and thermal sensations (Craig, 2003*a*, *b*). It has been proposed that altered interoception and anxiety are linked and that individuals prone to anxiety are associated with exaggerated interoceptive prediction signals generated in the anterior insula (Paulus and Stein, 2006). Because the posterior insula provides direct inputs to its anterior part, structural abnormalities of the posterior insula may adversely affect the function of the anterior insula, which contributes to anxiety-related symptoms of PFX$^+$ and PFX$^-$. In the present correlation analysis, although the correlation between level of obsessive–compulsiveness and reduced insula volume was significant bilaterally at an uncorrected threshold, it did not reach the significant level after correction. More observations are needed to test the possible association between the grey matter loss in the insula and anxiety-related symptoms of the premutation carriers.

Significant grey matter loss of PFX$^+$ was also identified in the medial temporal lobe structures including parts of the fusiform gyrus and parahippocampus. Abnormalities were more extended in the left hemisphere, involving the hippocampus and amygdala. Although a number of studies indicated the pathological processes of depression in the hippocampus (Soares and Mann, 1997; Sheline, 2000), correlation between left hippocampal grey matter density and the severity of depressive symptom was marginally significant only when an uncorrected threshold was used. Previous neuropsychological and functional imaging studies have shown the critical role of the left hippocampus in verbal memory (Milner, 1972; Strange *et al.*, 1999). Structural abnormalities of this area may therefore underlie impaired declarative verbal memory in PFX$^+$ (Grigsby *et al.*, 2008), although this possibility needs to be examined more directly by analysis using behavioural measures of declarative memory. In contrast, we observed a clear negative correlation between the left amygdala volume and elevated levels of obsessive–compulsiveness and depression. Together with our previous functional MRI study that found functional abnormalities in the amygdala in PFX$^-$ (Hessl *et al.*, 2007), this finding further supports the view that abnormalities in the amygdala play crucial roles in psychological symptoms of *FMR1* premutation carriers. It is interesting that the left amygdala underlies both depression and an anxiety-related symptom, given a high comorbidity between depression and anxiety disorders (Kessler *et al.*, 2003). Our result is consistent with previous findings of pathological processes affecting structure and function of the amygdala in patients with the obsessive–compulsive disorder (Szeszko *et al.*, 1999; Menzies *et al.*, 2008) and in those with depression (Sheline, 2000).

As predicted from neuropsychological observations, significant clusters of grey matter loss of the patient group were found in multiple areas for executive cognitive functions and working memory, including the inferior frontal cortex, dorsolateral prefrontal cortex and superior parietal cortex (Figs 1 and 3; Table 2). Significant correlations between left inferior frontal cortex volume and working memory scores indicates that grey matter loss in this region, together with that in the anterior cingulate cortex, contributes to working memory deficits in PFX$^+$ and in PFX$^-$ (Grigsby *et al.*, 2008; Cornish *et al.*, 2009) (Fig. 3). A previous behavioural study demonstrated significant impairment in response inhibition in both affected and unaffected premutation carriers (Cornish *et al.*, 2008). Although past brain lesion and functional imaging studies replicated the pivotal roles of the right inferior frontal cortex in response inhibition (Konishi *et al.*, 1999; Aron *et al.*, 2004), we did not observe significant voxels with grey matter reduction of PFX$^+$ in this region. It still remains possible that abnormalities of this region may be more apparent in the functional measures rather than the structural ones. Furthermore, response inhibition is subserved by connectivity between the right inferior frontal cortex and other brain regions including the striatum (Aron and Poldrack, 2006). It would be interesting to examine in the future studies the structural and functional connectivity between the right inferior frontal cortex and other regions.

Although extensive grey matter atrophy was identified in PFX$^+$, neuropsychological studies have widely reported cognitive functions that remain preserved or only mildly impaired (Cornish *et al.*, 2008; Grigsby *et al.*, 2008). In particular, language impairments have not been reported for any of the 16 subscales for 'language' and 'verbal reasoning and comprehension' (Grigsby *et al.*, 2008). In the voxel-based analysis, however, a rather significant increase of grey matter density for the patient group was

identified in the bilateral posterior part of superior/middle temporal gyrus. Although this observation has several possible explanations, the structural increase may play compensatory roles for maintaining language functions despite neurodegenerative processes affecting other language-related regions including the left inferior frontal cortex (Figs 1 and 3). Visuospatial functions and visual attention were suggested to be only mildly impaired in PFX^+ (Grigsby *et al.*, 2008). The present voxel-based analysis revealed significant grey matter reduction in some regions of the visuospatial and dorsal visual systems, such as the right superior parietal cortex, whereas the other regions of these systems, including the right superior occipital gyrus, did not have voxels with significant grey matter reduction. It is possible that there is a functional change in intact regions that compensates for structural degeneration affecting other parts of the systems.

In addition to atrophy affecting grey matter, importance of pathological changes in the white matter has been increasingly recognized in many neurological and psychiatric conditions (Kanaan *et al.*, 2005; Stebbins and Murphy, 2009). Indeed, hyperintensities in the periventricular and cerebellar zones have been recognized as one of the hallmark neuroradiological features of the FXTAS brain (Brunberg *et al.*, 2002). Because the present analyses focused on alternations of grey matter, it remains unanswered how the white matter abnormalities are related to the FXTAS symptomatology and *FMR1* molecular variables. The use of the MRI sequences optimal for the white matter pathology, such as the diffusion tensor imaging and the fluid-attenuated inversion recovery sequence, would complement our present findings of the grey matter abnormalities for better understanding of brain abnormalities in PFX^+.

To conclude, the current voxel-based morphometry study revealed the pattern of regional grey matter abnormalities of PFX^+ over the whole brain that may underlie its behavioural problems in the motor, cognitive and psychiatric domains. Findings of group comparisons together with regression analyses using *FMR1* genetic molecular variables and a clinical severity scale provide foundations at the systems-level for bridging the gap between genetic molecular pathological processes and clinical behavioural observations.

Funding

The National Institute of Health grants (UL1DE019583, DA024854 and HD036071); National Institute on Neurological Disorders and Stroke grant (RL1NS062412); National Institute on Ageing grants (RL1AG032119 and RL1AG032115); National Centre for Research Resources (UL1 RR024146); Roche, Novartis, Seaside Therapeutics, Forest, Johnson and Johnson, and Neuropharm, treatment trials in fragile X or autism (to R.J.H.).

References

Adams JS, Adams PE, Nguyen D, Brunberg JA, Tassone F, Zhang W, et al. Volumetric brain changes in females with fragile X-associated tremor/ataxia syndrome (FXTAS). Neurology 2007; 69: 851–9.

Adams PE, Adams JS, Nguyen DV, Hessl D, Brunberg JA, Tassone F, et al. Psychological symptoms correlate with reduced hippocampal volume in fragile X premutation carriers. Am J Med Genet B Neuropsychiatr Genet 2010; 153B: 775–85.

Aron AR, Monsell S, Sahakian BJ, Robbins TW. A componential analysis of task-switching deficits associated with lesions of left and right frontal cortex. Brain 2004; 127 (Pt 7): 1561–73.

Aron AR, Poldrack RA. Cortical and subcortical contributions to Stop signal response inhibition: role of the subthalamic nucleus. J Neurosci 2006; 26: 2424–33.

Ashburner J, Friston KJ. Voxel-based morphometry—the methods. Neuroimage 2000; 11 (6 Pt 1): 805–21.

Ashburner J, Friston KJ. Unified segmentation. Neuroimage 2005; 26: 839–51.

Augustine JR. Circuitry and functional aspects of the insular lobe in primates including humans. Brain Res Brain Res Rev 1996; 22: 229–44.

Bacalman S, Farzin F, Bourgeois JA, Cogswell J, Goodlin-Jones BL, Gane LW, et al. Psychiatric phenotype of the fragile X-associated tremor/ataxia syndrome (FXTAS) in males: newly described fronto-subcortical dementia. J Clin Psychiatry 2006; 67: 87–94.

Bechara A, Damasio H, Damasio AR. Emotion, decision making and the orbitofrontal cortex. Cereb Cortex 2000; 10: 295–307.

Beckmann M, Johansen-Berg H, Rushworth MF. Connectivity-based parcellation of human cingulate cortex and its relation to functional specialization. J Neurosci 2009; 29: 1175–90.

Benjamini Y, Hochberg Y. Controlling the false discovery rate: a practical and powerful approach to multiple testing. J R Stat Soc 1995; 57: 289–300.

Berry-Kravis E, Abrams L, Coffey SM, Hall DA, Greco C, Gane LW, et al. Fragile X-associated tremor/ataxia syndrome: clinical features, genetics, and testing guidelines. Mov Disord 2007a; 22: 2018–30.

Berry-Kravis E, Goetz CG, Leehey MA, Hagerman RJ, Zhang L, Li L, et al. Neuropathic features in fragile X premutation carriers. Am J Med Gene 2007b; 143: 19–26.

Bourgeois JA, Coffey SM, Rivera SM, Hessl D, Gane LW, Tassone F, et al. A review of fragile X premutation disorders: expanding the psychiatric perspective. J Clin Psychiatry 2009; 70: 852–62.

Bourgeois JA, Cogswell JB, Hessl D, Zhang L, Ono MY, Tassone F, et al. Cognitive, anxiety and mood disorders in the fragile X-associated tremor/ataxia syndrome. Gen Hosp Psychiatry 2007; 29: 349–56.

Brunberg JA, Jacquemont S, Hagerman RJ, Berry-Kravis EM, Grigsby J, Leehey MA, et al. Fragile X premutation carriers: characteristic MR imaging findings of adult male patients with progressive cerebellar and cognitive dysfunction. AJNR Am J Neuroradiol 2002; 23: 1757–66.

Buckner RL, Koutstaal W. Functional neuroimaging studies of encoding, priming, and explicit memory retrieval. Proc Natl Acad Sci USA 1998; 95: 891–8.

Bush G, Luu P, Posner MI. Cognitive and emotional influences in anterior cingulate cortex. Trends Cogn Sci 2000; 4: 215–22.

Cabeza R, Nyberg L. Imaging cognition II: an empirical review of 275 PET and fMRI studies. J Cogn Neurosci 2000; 12: 1–47.

Cavada C, Company T, Tejedor J, Cruz-Rizzolo RJ, Reinoso-Suarez F. The anatomical connections of the macaque monkey orbitofrontal cortex. A review. Cereb Cortex 2000; 10: 220–42.

Cavanna AE, Trimble MR. The precuneus: a review of its functional anatomy and behavioural correlates. Brain 2006; 129 (Pt 3): 564–83.

Chamberlain SR, Menzies L, Hampshire A, Suckling J, Fineberg NA, del Campo N, et al. Orbitofrontal dysfunction in patients with obsessive-compulsive disorder and their unaffected relatives. Science 2008; 321: 421–2.

Chen Y, Tassone F, Berman RF, Hagerman PJ, Hagerman RJ, Willemsen R, et al. Murine hippocampal neurons expressing Fmr1 gene premutations show early developmental deficits and late degeneration. Hum Mol Genet 2010; 19: 196–208.

Cohen S, Masyn K, Adams J, Hessl D, Rivera S, Tassone F, et al. Molecular and imaging correlates of the fragile X-associated tremor/ataxia syndrome. Neurology 2006; 67: 1426–31.

Cornish KM, Kogan CS, Li L, Turk J, Jacquemont S, Hagerman RJ. Lifespan changes in working memory in fragile X premutation males. Brain Cogn 2009; 69: 551–8.
Cornish KM, Li L, Kogan CS, Jacquemont S, Turk J, Dalton A, et al. Age-dependent cognitive changes in carriers of the fragile X syndrome. Cortex 2008; 44: 628–36.
Cornish K, Kogan C, Turk J, Manly T, James N, Mills A, et al. The emerging fragile X premutation phenotype: evidence from the domain of social cognition. Brain Cogn 2005; 57: 53–60.
Craig AD. Interoception: the sense of the physiological condition of the body. Curr Opin Neurobiol 2003a; 13: 500–5.
Craig AD. A new view of pain as a homeostatic emotion. Trends Neurosci 2003b; 26: 303–7.
Derogatis L. Symptom checklist-90-R: Adminstration, scoring, and procedures manual. 3rd edition, Minneapolis: National Compuer Systems, Inc.; 1994.
Diener Healthy Control, Dichgans J, Guschlbauer B, Bacher M, Langenbach P. Disturbances of motor preparation in basal ganglia and cerebellar disorders. Prog Brain Res 1989; 80: 481–8.
Etkin A, Wager TD. Functional neuroimaging of anxiety: a meta-analysis of emotional processing in PTSD, social anxiety disorder, and specific phobia. Am J Psychiatry 2007; 164: 1476–88.
Farzin F, Perry H, Hessl D, Loesch D, Cohen J, Bacalman S, et al. Autism spectrum disorders and attention-deficit/hyperactivity disorder in boys with the fragile X premutation. J Dev Behav Pediatr 2006; 27 (2 Suppl.): S137–44.
Franke P, Leboyer M, Gansicke M, Weiffenbach O, Biancalana V, Cornillet-Lefebre P, et al. Genotype-phenotype relationship in female carriers of the premutation and full mutation of FMR-1. Psychiatry Res 1998; 80: 113–27.
Fu YH, Kuhl DP, Pizzuti A, Pieretti M, Sutcliffe JS, Richards S, et al. Variation of the CGG repeat at the fragile X site results in genetic instability: resolution of the Sherman paradox. Cell 1991; 67: 1047–58.
Garcia-Arocena D, Hagerman PJ. Advances in understanding the molecular basis of FXTAS. Hum Mol Genet 2010; 19: R83–9.
Greco CM, Berman RF, Martin RM, Tassone F, Schwartz PH, Chang A, et al. Neuropathology of fragile X-associated tremor/ataxia syndrome (FXTAS). Brain 2006; 129 (Pt 1): 243–55.
Greco CM, Hagerman RJ, Tassone F, Chudley AE, Del Bigio MR, Jacquemont S, et al. Neuronal intranuclear inclusions in a new cerebellar tremor/ataxia syndrome among fragile X carriers. Brain 2002; 125 (Pt 8): 1760–71.
Greicius MD, Krasnow B, Reiss AL, Menon V. Functional connectivity in the resting brain: a network analysis of the default mode hypothesis. Proc Natl Acad Sci USA 2003; 100: 253–8.
Grigsby J, Brega AG, Engle K, Leehey MA, Hagerman RJ, Tassone F, et al. Cognitive profile of fragile X premutation carriers with and without fragile X-associated tremor/ataxia syndrome. Neuropsychology 2008; 22: 48–60.
Grigsby J, Brega AG, Jacquemont S, Loesch DZ, Leehey MA, Goodrich GK, et al. Impairment in the cognitive functioning of men with fragile X-associated tremor/ataxia syndrome (FXTAS). J Neurol Sci 2006; 248: 227–33.
Grigsby J, Brega AG, Leehey MA, Goodrich GK, Jacquemont S, Loesch DZ, et al. Impairment of executive cognitive functioning in males with fragile X-associated tremor/ataxia syndrome. Mov Disord 2007; 22: 645–50.
Gusnard DA, Raichle ME. Searching for a baseline: functional imaging and the resting human brain. Nat Rev Neurosci 2001; 2: 685–94.
Habas C, Kamdar N, Nguyen D, Prater K, Beckmann CF, Menon V, et al. Distinct cerebellar contributions to intrinsic connectivity networks. J Neurosci 2009; 29: 8586–94.
Hagerman RJ, Hagerman PJ. The fragile X premutation: into the phenotypic fold. Curr Opin Genet Dev 2002; 12: 278–83.
Hagerman PJ, Hagerman RJ. Fragile X-associated tremor/ataxia syndrome (FXTAS). Ment Retard Dev Disabil Res Rev 2004; 10: 25–30.
Hagerman RJ, Leehey M, Heinrichs W, Tassone F, Wilson R, Hills J, et al. Intention tremor, parkinsonism, and generalized brain atrophy in male carriers of fragile X. Neurology 2001; 57: 127–30.
Hessl D, Rivera S, Koldewyn K, Cordeiro L, Adams J, Tassone F, et al. Amygdala dysfunction in men with the fragile X premutation. Brain 2007; 130 (Pt 2): 404–16.
Hessl D, Tassone F, Loesch DZ, Berry-Kravis E, Leehey MA, Gane LW, et al. Abnormal elevation of FMR1 mRNA is associated with psychological symptoms in individuals with the fragile X premutation. Am J Med Genet B Neuropsychiatr Genet 2005; 139B: 115–21.
Jacquemont S, Hagerman RJ, Leehey M, Grigsby J, Zhang L, Brunberg JA, et al. Fragile X premutation tremor/ataxia syndrome: molecular, clinical, and neuroimaging correlates. Am J Hum Genet 2003; 72: 869–78.
Johnston C, Eliez S, Dyer-Friedman J, Hessl D, Glaser B, Blasey C, et al. Neurobehavioral phenotype in carriers of the fragile X premutation. Am J Med Genet 2001; 103: 314–9.
Kanaan RA, Kim JS, Kaufmann WE, Pearlson GD, Barker GJ, McGuire PK. Diffusion tensor imaging in schizophrenia. Biol Psychiatry 2005; 58: 921–9.
Kaye K, Grigsby J, Robbins LJ, Korzun B. Prediction of independent functioning and behavior problems in geriatric patients. J Am Geriatr Soc 1990; 38: 1304–10.
Kennedy DP, Redcay E, Courchesne E. Failing to deactivate: resting functional abnormalities in autism. Proc Natl Acad Sci USA 2006; 103: 8275–80.
Kenneson A, Zhang F, Hagedorn CH, Warren ST. Reduced FMR1 protein and increased FMR1 transcription is proportionally associated with CGG repeat number in intermediate-length and premutation carriers. Hum Mol Genet 2001; 10: 1449–54.
Kessler RC, Berglund P, Demler O, Jin R, Koretz D, Merikangas KR, et al. The epidemiology of major depressive disorder: results from the National Comorbidity Survey Replication (NCS-R). Jama 2003; 289: 3095–105.
Konishi S, Nakajima K, Uchida I, Kikyo H, Kameyama M, Miyashita Y. Common inhibitory mechanism in human inferior prefrontal cortex revealed by event-related functional MRI. Brain 1999; 122 (Pt 5): 981–91.
Kringelbach ML. The human orbitofrontal cortex: linking reward to hedonic experience. Nat Rev Neurosci 2005; 6: 691–702.
Kuperberg GR, Broome MR, McGuire PK, David AS, Eddy M, Ozawa F, et al. Regionally localized thinning of the cerebral cortex in schizophrenia. Arch Gen Psychiatry 2003; 60: 878–88.
Lasek K, Lencer R, Gaser C, Hagenah J, Walter U, Wolters A, et al. Morphological basis for the spectrum of clinical deficits in spinocerebellar ataxia 17 (SCA17). Brain 2006; 129 (Pt 9): 2341–52.
Leehey MA, Berry-Kravis E, Min SJ, Hall DA, Rice CD, Zhang L, et al. Progression of tremor and ataxia in male carriers of the FMR1 premutation. Mov Disord 2007; 22: 203–6.
Loesch DZ, Churchyard A, Brotchie P, Marot M, Tassone F. Evidence for, and a spectrum of, neurological involvement in carriers of the fragile X pre-mutation: FXTAS and beyond. Clin Genet 2005; 67: 412–7.
Maldjian JA, Laurienti PJ, Kraft RA, Burdette JH. An automated method for neuroanatomic and cytoarchitectonic atlas-based interrogation of fMRI data sets. Neuroimage 2003; 19: 1233–9.
Menzies L, Chamberlain SR, Laird AR, Thelen SM, Sahakian BJ, Bullmore ET. Integrating evidence from neuroimaging and neuropsychological studies of obsessive-compulsive disorder: the orbitofronto-striatal model revisited. Neurosci Biobehav Rev 2008; 32: 525–49.
Milner B. Disorders of learning and memory after temporal lobe lesions in man. Clin Neurosurg 1972; 19: 421–46.
Monk CS, Peltier SJ, Wiggins JL, Weng SJ, Carrasco M, Risi S, et al. Abnormalities of intrinsic functional connectivity in autism spectrum disorders. Neuroimage 2009; 47: 764–72.
Moore CJ, Daly EM, Tassone F, Tysoe C, Schmitz N, Ng V, et al. The effect of pre-mutation of X chromosome CGG trinucleotide repeats on brain anatomy. Brain 2004; 127 (Pt 12): 2672–81.

Nakamura M, Nestor PG, Levitt JJ, Cohen AS, Kawashima T, Shenton ME, et al. Orbitofrontal volume deficit in schizophrenia and thought disorder. Brain 2008; 131 (Pt 1): 180–95.

Olichney JM, Chan S, Wong LM, Schneider A, Seritan A, Niese A, et al. Abnormal N400 word repetition effects in fragile X-associated tremor/ataxia syndrome. Brain 2010; 133 (Pt 5): 1438–50.

Ouchi Y, Okada H, Yoshikawa E, Nobezawa S, Futatsubashi M. Brain activation during maintenance of standing postures in humans. Brain 1999; 122 (Pt 2): 329–38.

Paulus MP, Stein MB. An insular view of anxiety. Biol Psychiatry 2006; 60: 383–7.

Paus T. Primate anterior cingulate cortex: where motor control, drive and cognition interface. Nat Rev Neurosci 2001; 2: 417–24.

Pieretti M, Zhang FP, Fu YH, Warren ST, Oostra BA, Caskey CT, et al. Absence of expression of the FMR-1 gene in fragile X syndrome. Cell 1991; 66: 817–22.

Raichle ME, MacLeod AM, Snyder AZ, Powers WJ, Gusnard DA, Shulman GL. A default mode of brain function. Proc Natl Acad Sci USA 2001; 98: 676–82.

Rushworth MF, Behrens TE, Rudebeck PH, Walton ME. Contrasting roles for cingulate and orbitofrontal cortex in decisions and social behaviour. Trends Cogn Sci 2007; 11: 168–76.

Schmahmann JD, Doyon J, McDonald D, Holmes C, Lavoie K, Hurwitz AS, et al. Three-dimensional MRI atlas of the human cerebellum in proportional stereotaxic space. Neuroimage 1999; 10 (3 Pt 1): 233–60.

Schmahmann JD, Sherman JC. The cerebellar cognitive affective syndrome. Brain 1998; 121 (Pt 4): 561–79.

Sheline YI. 3D MRI studies of neuroanatomic changes in unipolar major depression: the role of stress and medical comorbidity. Biol Psychiatry 2000; 48: 791–800.

Smith EE, Jonides J. Storage and executive processes in the frontal lobes. Science 1999; 283: 1657–61.

Soares JC, Mann JJ. The anatomy of mood disorders—review of structural neuroimaging studies. Biol Psychiatry 1997; 41: 86–106.

Soontarapornchai K, Maselli R, Fenton-Farrell G, Tassone F, Hagerman PJ, Hessl D, et al. Abnormal nerve conduction features in fragile X premutation carriers. Arch Neurol 2008; 65: 495–8.

Stebbins GT, Murphy CM. Diffusion tensor imaging in Alzheimer's disease and mild cognitive impairment. Behav Neurol 2009; 21: 39–49.

Stoodley CJ, Schmahmann JD. Functional topography in the human cerebellum: a meta-analysis of neuroimaging studies. Neuroimage 2009; 44: 489–501.

Strange BA, Fletcher PC, Henson RN, Friston KJ, Dolan RJ. Segregating the functions of human hippocampus. Proc Natl Acad Sci USA 1999; 96: 4034–9.

Szeszko PR, Robinson D, Alvir JM, Bilder RM, Lencz T, Ashtari M, et al. Orbital frontal and amygdala volume reductions in obsessive-compulsive disorder. Arch Gen Psychiatry 1999; 56: 913–9.

Tassone F, Adams J, Berry-Kravis EM, Cohen SS, Brusco A, Leehey MA, et al. CGG repeat length correlates with age of onset of motor signs of the fragile X-associated tremor/ataxia syndrome (FXTAS). Am J Med Genet B Neuropsychiatr Genet 2007; 144B: 566–9.

Tassone F, Pan R, Amiri K, Taylor AK, Hagerman PJ. A rapid polymerase chain reaction-based screening method for identification of all expanded alleles of the fragile X (FMR1) gene in newborn and high-risk populations. J Mol Diagn 2008; 10: 43–9.

Tassone F, Iwahashi C, Hagerman PJ. FMR1 RNA within the intranuclear inclusions of fragile X-associated tremor/ataxia syndrome (FXTAS). RNA biology 2004; 1: 103–5.

Tassone F, Hagerman RJ, Taylor AK, Gane LW, Godfrey TE, Hagerman PJ. Elevated levels of FMR1 mRNA in carrier males: a new mechanism of involvement in the fragile-X syndrome. Am J Hum Genet 2000; 66: 6–15.

Verkerk AJ, Pieretti M, Sutcliffe JS, Fu YH, Kuhl DP, Pizzuti A, et al. Identification of a gene (FMR-1) containing a CGG repeat coincident with a breakpoint cluster region exhibiting length variation in fragile X syndrome. Cell 1991; 65: 905–14.

Vogt BA, Nimchinsky EA, Vogt LJ, Hof PR. Human cingulate cortex: surface features, flat maps, and cytoarchitecture. J Comp Neurol 1995; 359: 490–506.